Inorganica Chimica Acta, *173* (1990) 247–254

New Route to Bimetallic Imidazole-bridged Complexes

IV. Synthesis and Characterization of Homobinuclear (Cu–Cu; Ni–Ni) and Heterobinuclear (Cu–Ni; Cu–Zn; Ni–Zn) Imidazolate-bridged Complexes from Novel Mononuclear Entities

JEAN-PIERRE COSTES*

Laboratoire de Chimie de Coordination du CNRS, UP 8241 liée par conventions à l'Université Paul Sabatier et à l'Institut National Polytechnique, 205 Route de Narbonne, 31077 Toulouse Cédex (France)

and M. I. FERNANDEZ-GARCIA

Colegio Universitario de Lugo, Universidad de Santiago de Compostela (Spain)

(Received November 20, 1989; revised February 8, 1990)

Abstract

A novel non-symmetrical tetradentate Schiff base, AE-ImH, resulting from the condensation of 7-amino-4-methyl-5-aza-3-hepten-2-one (AEH) with imidazole-2-carboxaldehyde, has been prepared and characterized. This ligand can react with copper and nickel ions to yield neutral $M_iAE\text{-}Im$ entities. When M_i is Cu, the mononuclear units are associated in the solid state to yield a chain structure. Subsequent reaction of the mononuclear units with M_oAE entities (M_i for inner, M_o for outer metal coordination site relating to the AE-ImH ligand) or $Zn(hfa)_2\cdot2H_2O$ (hfa = anion of hexafluoroacetylacetone) gave homo- (Cu–Cu; Ni–Ni) and heterobinuclear (Cu–Ni; Cu–Zn; Ni–Zn) imidazolate-bridged complexes $[M_iAE\text{-}ImM_oAE]^+$ or $M_iAE\text{-}ImZn(hfa)_2$. A significant antiferromagnetic interaction is operative in the copper–copper complex ($2J = -48$ cm^{-1}; $g = 2.08$). NMR, ESR and electronic spectra confirm the existence of the dinuclear structure in solution. From the entire set of results we may assume that in the dinuclear complexes, the imidazolate ligand has a rather localized structure with two markedly different nitrogen atoms, viz. a pyrrolic nitrogen at the inner site and a pyridinic nitrogen at the outer site.

Introduction

Mononuclear complexes able to act as ligands toward other metal ions are of current interest. Most of the reported 'ligand-complexes' are derived from symmetrical Schiff bases and behave as bidentate ligands. However monodentate 'ligand-complexes' have been recently reported [1–8]. They are obtained from unsymmetrical quadridentate ligands which comprise an imidazole moiety in their structure. The ligands considered in this work belong to this general type but the binding of the imidazole fragment to the rest of the molecule is through the C(2) atom, as in ref. 5, and not through the C(4) atom as it is in the other previously reported examples.

Reaction of the 'half-unit' AEH, 7-amino-4-methyl-5-aza-3-hepten-2-one with imidazole-2-carboxaldehyde results in the formation of an AE-ImH ligand which offers a N_3O coordination site to a first metal ion while the outer nitrogen atom of the imidazole fragment remains free and therefore able to link a second metal ion. Mononuclear (MAE-Im) (**A**) units, homo- and heterobinuclear complexes ($[M_iAE\text{-}ImM_oAE]^+$ (**B**) or $MAE\text{-}ImZn(hfa)_2$ (**C**)) have been obtained in this way. They are represented in Fig. 1 together with two series of related complexes, $[AEMImH]^+$ and $[AEMImM'AE]^+$, which have been previously described [9–11].

There are two types of imidazolate-bridged complexes in the literature. In the first one, the two sites of coordination are identical, as in $[AEMImMAE]^+$ [9], while in the second one they are very different, as in ref. 7. In the present paper, we have an intermediate case where the two coordination sites appear to be nearly similar at first sight, for M_i and M_o are in a N_3O environment. Despite this fact, the physical properties confirm that the two sites are really different and that such a little difference can strongly modify the ligand field around each metal atom.

In the following, the usual ligands, pyridine, pyrrole, imidazole and imidazolate are represented by Py, Pyr, ImH, and Im, respectively.

---

*Author to whom correspondence should be addressed.

0020-1693/90/$3.50

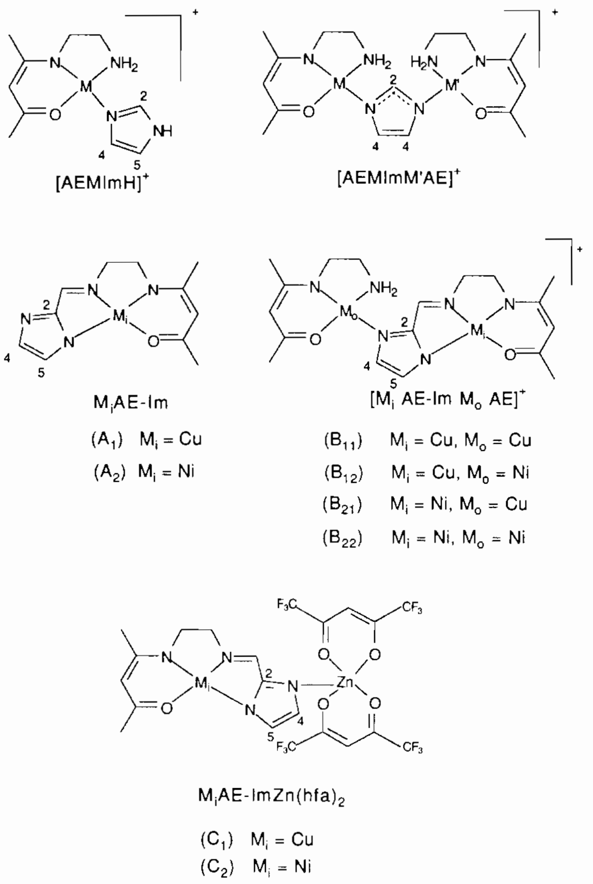

The subscripts i and o are used to distinguish the inner site M$_i$ from the outer site M$_o$
2, 4, 5 indicate the NMR numbering of the imidazole rings

Fig. 1. Schematic structure of the monomeric and dimeric species with NMR numbering of the imidazole rings.

Experimental

Ligand AE-ImH

To AEH (7-amino-4-methyl-5-aza-3-hepten-2-one) [12] (1 g; 7.04×10^{-3} M) in MeOH (40 ml) was added imidazole-2-carboxaldehyde (0.67 g; 7.04×10^{-3} M). The mixture was stirred and heated for 30 min. The cold solution was evaporated under reduced pressure yielding a white precipitate which was washed with Et_2O and dried. *Anal.* Calc. for $C_{11}H_{16}N_4O$: C, 60.0; H, 7.3; N, 25.4. Found: C, 60.1; H, 7.6; N, 25.1%.

Mononuclear Units

CuAE-Im (A_1) and NiAE-Im (A_2) were obtained by mixing of the ligand and $CuAc_2H_2O$ or $NiAc_2H_2O$ (Ac = acetate) in MeOH in the presence of NEt_3 (nickel case) or without (copper case) as previously published [13] for a similar ligand.

These units could be prepared in one step with the following procedure. To [AENiPy]ClO_4 [14] (1 g; 2.6×10^{-3} M) in MeOH (40 ml) were added imidazole-2-carboxaldehyde (0.25 g, 2.6×10^{-3} M) and NaOH (0.21 g in 15 ml of water). The mixture was refluxed for 30 min and the solution was then reduced to 25 ml. Addition of water (60 ml) induced the appearance of a yellow precipitate which was filtered, washed with MeOH, Et_2O and dried. Yield: 80%. *Anal.* Calc. for $C_{11}H_{14}N_4NiO \cdot 2H_2O$: C, 42.3; H, 5.8; N, 17.9. Found: C, 42.2; H, 5.7; N, 17.5%.

Starting with [AE Cu Py]ClO_4 yielded the copper entity with an identical yield. *Anal.* Calc. for $C_{11}H_{14}CuN_4O \cdot H_2O$: C, 44.1; H, 5.3; N, 18.7. Found: C, 44.2; H, 5.3; N, 18.3%.

AECuNCS and AENiNCS

To an ethanolic solution (50 ml) of AEH (1 g; 7.0×10^{-3} M), KSCN (0.7 g; 7.10^{-3} M) and NEt_3 (0.7 g; 7.0×10^{-3} M) was added an ethanolic solution (20 ml) of $Ni(NO_3)_2$, $6H_2O$ (2 g; 7.0×10^{-3} M). The mixture turned orange and a precipitate appeared in a few minutes. The filtered product was dissolved in boiling acetone. From the filtrate, left overnight, orange–red crystals precipitated which were filtered and dried. *Anal.* Calc. for $C_8H_{13}N_3NiOS$: C, 37.3; H, 5.1; N, 16.3. Found: C, 37.0; H, 5.2; N, 16.1%.

AECuNCS was obtained similarly. *Anal.* Calc. for $C_8H_{13}CuN_3OS$: C, 36.6; H, 5.0; N, 16.0. Found: C, 36.4; H, 5.1; N, 15.7%.

Bimetallic Species

[MAE-ImM'AE]ClO$_4$ species

These complexes were obtained using the following experimental procedure. To the monometallic entity MAE-Im (10^{-3} M) in MeOH (30 ml) were successively added AEM'NCS (10^{-3} M) in MeOH (20 ml) and $NaClO_4$ (0.2 g). The solution was heated for 30 min with stirring, then concentrated to half-volume. The precipitate was filtered, washed with MeOH, Et_2O and dried.

[CuAE-ImCuAE]ClO$_4$·2H$_2$O (B$_{11}$)

This product was prepared by the use of [AECuAc]$_2$ [15] instead of AECuNCS. Yield: 70%. *Anal.* Calc. for $C_{18}H_{27}ClCu_2N_6O_6 \cdot 2H_2O$: C, 34.7; H, 5.0; Cu, 20.4; N, 13.5. Found: C, 34.3; H, 5.2; Cu, 20.0; N, 13.3%.

[CuAE-ImNiAE]ClO$_4$·2H$_2$O (B$_{12}$)

Yield: 75%. *Anal.* Calc. for $C_{18}H_{27}ClCuN_6NiO_6 \cdot 2H_2O$: C, 35.1; H, 5.0; Cu, 10.3; N, 13.6; Ni, 9.4. Found: C, 35.0; H, 5.1; Cu, 10.0; N, 13.7; Ni, 9.2%.

[NiAE-ImCuAE]ClO$_4$·2H$_2$O (B$_{21}$)

Yield: 77%. *Anal.* Calc. for $C_{18}H_{27}ClCuN_6NiO_6 \cdot 2H_2O$: C, 35.1; H, 5.0; Cu, 10.3; N, 13.6; Ni, 9.4. Found: C, 34.9; H, 5.3; Cu, 10.1; N, 13.3; Ni, 9.4%.

[NiAE-ImNiAE]ClO₄ (B₂₂)

Yield: 80%. *Anal.* Calc. for $C_{18}H_{27}ClN_6Ni_2O_6 \cdot 2H_2O$: C, 35.4; H, 5.0; N, 13.7; Ni, 19.0. Found: C, 35.0; H, 5.2; N, 13.5; Ni, 18.7%.

NiAE-ImZn(hfa)₂·2H₂O (C₂)

To NiAE-Im (0.1 g; 3.4×10^{-4} M) in MeOH (20 ml) was added $Zn(hfa)_2 \cdot 2H_2O$ (0.17 g; 3.4×10^{-4} M). From the resulting solution stirred for 4 h appeared a yellow precipitate which was filtered, washed (MeOH, Et_2O) and dried. Yield 85%. *Anal.* Calc. for $C_{21}H_{16}F_{12}N_4NiO_5Zn \cdot 2H_2O$: C, 32.0; H, 2.5; N, 7.1; Ni, 7.3; Zn, 8.2. Found: C, 31.7; H, 2.6; N, 7.0; Ni, 7.2; Zn, 8.1%.

CuAE-ImZn(hfa)₂·2H₂O (C₁)

This was prepared similarly but no precipitate appeared from the solution. Therefore the methanol was evaporated and the precipitate was dissolved in Et_2O and filtered. Addition of pentane induced the precipitation of a raspberry red product which was filtered and dried. Yield: 70%. *Anal.* Calc. for $C_{21}H_{16}CuF_{12}N_4O_5Zn \cdot 2H_2O$: C, 31.6; H, 2.5; N, 7.0; Cu, 8.0; Zn, 8.2. Found: C, 31.2; H, 2.6; N, 6.8; Cu, 7.8; Zn, 7.9%.

Physical Measurements

Electronic spectra were obtained with a Cary 2390 spectrometer. EPR spectra were recorded at X-band frequencies with a Bruker 200 TT spectrometer operating at 9.4–9.5 GHz. ^1H and ^{13}C NMR spectra were recorded at 299 K with a Bruker AC 200 spectrometer. All chemical shifts (^1H and ^{13}C) are given in ppm versus TMS. Magnetic susceptibility data were collected on powdered samples using a Faraday type magnetometer fitted with a helium continuous flow cryostat. Independence of the magnetic susceptibility versus magnetic field was checked at each temperature. Mercury tetrakis(thiocyanato) cobaltate (susceptibility at 20 °C: 16.44×10^{-6} cgsu) was used as a susceptibility standard. All data were corrected for diamagnetism (estimated at -112×10^{-6} cgsu for A_1 and -219×10^{-6} cgsu for B_{11}) and *TIP* (taken as 60×10^{-6} cgsu/Cu atom). Magnetic susceptibility measurements of complexes in solution were determined by NMR [16] using pyridine as solvent and t-butanol as indicator.

Results and Discussion

As described in 'Experimental', the mononuclear units A_1 and A_2 may be obtained via two routes. The first one consists in reacting the preformed ligand AE-ImH with metallic salts in alcohol with or without addition of triethylamine. Triethylamine is not necessary to deprotonate the ligand but induces a better precipitation of the resulting complex at least in the case of nickel, as noticed elsewhere [13]. The second route relies on the template effect. A precursor such as $[AEMB]^+$ (M = Cu, Ni; B = Py, ImH) [10, 14] or [AEMNCS] and imidazole-2-carboxaldehyde are mixed together in alcohol. Addition of aqueous NaOH and then a short heating period yields the desired product. In any case, we did not succeed in obtaining the related non-deprotonated entity, $[MAE\text{-}ImH]^+$, even without use of any base in the experimental process. Other authors [4], who prepared a similar ligand with imidazole-4-carboxaldehyde instead of imidazole-2-carboxaldehyde, could isolate the mono and dideprotonated species. Furthermore, ligands formed by salicylaldehyde instead of 2,4-pentanedione, 1,3-diaminopropane instead of 1,2-diaminoethane and imidazole-4-carboxaldehyde also gave mono and dideprotonated complexes, while the use of imidazole-2-carboxaldehyde induced the formation of dideprotonated species [5].

In A_1 and A_2, one nitrogen atom of the imidazole ring remains formally uncoordinated and available for linking a second metal atom to yield homo- and heterobinuclear complexes, $M_iAE\text{-}ImM_oAE$ (B) and $MAE\text{-}ImZn(hfa)_2$ (C).

All the complexes have been characterized by chemical analysis. The data are consistent with a neutral formulation for the mononuclear entities A_1 and A_2 and the dinuclear complexes C_1 and C_2, i.e. MAE-Im and $MAE\text{-}ImZn(hfac)_2$, respectively, and with a cationic formulation for the dinuclear complexes, $[M_iAE\text{-}ImM_oAE]^+$. This was supported by conductivity measurements. The values obtained for methanolic solutions of B_{11}, B_{12}, B_{21} and B_{22} range from 75 to 85 Ω^{-1} cm^2 mol^{-1} as expected for 1:1 electrolytes while a zero value of Λ characterizes the other complexes and confirms that they are non-conducting species.

NMR Spectroscopy

Further characterization of the free ligand and its nickel complexes is obtained from NMR (^1H and ^{13}C) spectra. The data are quoted in Tables 1 and 2.

The attributions have been made based on the data previously obtained for $[AENiImH]^+$ and $[AENiImNiAE]^+$ [10, 13] and multi-resonance experiments. Although the overall appearance of the spectra supports the proposed formulation, some unexpected features deserve further comments.

The ^1H and ^{13}C spectra of AE-ImH in DMSO-d_6 display more signals than expected while the ^1H spectrum in $CDCl_3$ is normal. The influence of the solvent together with the feeble difference of shifts characterizing each pair of signals in DMSO-d_6 suggest that the differences of the spectra result from modifications of the hydrogen bonding scheme. A closed conformation stabilized by intramolecular hydrogen bonding would be favoured in $CDCl_3$

TABLE 1. ^{13}C NMR data

	NC–CH_3	OC–CH_3	NH–CH_2	N–CH_2	N=CH	CH	CO	CN	Im		
									2	4	5
AE-ImH (DMSO-d_6)	18.7 18.4	28.7 28.6	43.1 42.9	60.7 60.4	153.9 153.4	95.2 94.9	193.3 193.1	163.1	144.5 144.4	124.8[a]	124.8[a]
A_2 (DMSO-d_6)	20.8	24.3	53.5	55.6	158.7	100.1	175.2	165.8	n.o.[b]	126.9	131.3
B_{22} $(CD_3)_2CO$	20.7 20.3	23.6 23.2	43.9 54.7	54.3 56.3	158.3	100.0 100.6	176.4 175.1	166.7 166.4	n.o.	127.0	130.2

[a]Large. [b]n.o. = not observed.

TABLE 2. ^1H NMR data

	CH_3CO	CH_3CN	CH_2N(H)	CH_2N or CH_2NH_2	CH	N=CH	Imidazole ring		NH	NH_2
							4	5		
AE-ImH ($CDCl_3$)	1.93	1.99	3.55[a]	3.75[b]	4.98	8.24[c]	7.13	7.13	11.19	
AE-ImH (DMSO)	1.94 1.97	2.00 2.04	3.47–3.83[d]		5.03 5.06	8.30[e]	7.23 7.26	7.23 7.26	10.77	
A_2 $(CD_3)_2CO$	1.87	2.04	3.54–3.75[d]		5.08	7.71	7.05	6.75		
A_2 (DMSO)	1.97	2.11	3.57–3.66[d]		5.25	7.94	7.07	6.69		
B_{22} (DMSO)	1.90[e] 1.99	2.05	3.72	3.72	5.05[e] 5.31	8.40	7.50	6.93		
B_{22} $(CD_3)_2CO$	1.82 2.12	2.02 2.20	3.41 3.88	2.70 3.88	5.11 5.31	8.50	7.25	6.84		2.90
C_2 (DMSO)	1.99	2.13	3.67	3.67	5.28 5.63[f]	7.91	7.10	6.76		

[a]Quartet J = 5.5 Hz. [b]Doublet of triplet. [c]Triplet J = 1.4 Hz. [d]Complex multiplet. [e]Large. [f]CH from hfa.

whereas a solvent able to compete with the internal acceptors would allow the presence of a second conformation.

As for the dinuclear complex $\mathbf{B}_{22}$, the ^1H and ^{13}C spectra in $(CD_3)_2CO$ show the presence of two inequivalent AE moieties since two sets of signals of very similar intensities and widths are observed. At first sight, the use of DMSO-d_6 results in a much simpler ^1H spectrum with only one set of signals. A careful examination shows that the second set has not vanished but has suffered modifications of the chemical shifts and widths of its signals. These effects are very likely attributable to coordination of the solvent DMSO onto one of the nickel atoms, giving rise to paramagnetic effects for the nuclei surrounding the metal coordinated to DMSO. However, broadening of the N=CH and C(4)H signals are also observed in $(CD_3)_3CO$. This is probably due to steric constraints which would prevent free rotation of the outer NiAE entity.

To support the hypothesis of paramagnetic effects related to the use of DMSO-d_6 as solvent, we have performed an independent experiment. Successive amounts of pyridine were added to an acetone solution of $\mathbf{B}_{22}$. The resulting ^1H spectra show that one group of signals was virtually unaffected while broadening and shifts were observed for the second group. The data are quoted in Table 3. Their interpretation is straightforward in keeping with the data previously obtained for the related system $[AENiImH]^+/Py$ [17] and a theoretical study of spin delocalization in a ligand similar to AEH [18]. The paramagnetic shifts (Δ) expected for the ^1H nuclei of an AE entity surrounding a high-spin nickel(II) are as follows: $\Delta(OC{-}CH_3)/\Delta(CH_2) = 0.02$ ppm, $\Delta(NC{-}CH_3)/\Delta(CH_2) = -0.16$ ppm, $\Delta(CH)/\Delta(CH_2) = -0.28$ ppm.

From Table 3 it is obvious that the signal nos. (1), (3), (6), (7) and (8) are respectively attributable to the OC–CH_3, NC–CH_3, CH_2 and CH nuclei of an AE

TABLE 3. Initial shifts (δ) and observed paramagnetic shifts (Δ) for $\mathbf{B}_{22}$

	Attribution	Initial shift δ	Observed paramagnetic shift Δ [a]
CH_3	(1)	1.82	0.03
	(2)	2.02	0.00
	(3)	2.13	−0.13
	(4)	2.22	−0.02
CH_2	(5)	3.88	−0.05
	(6)	2.71	1.00
	(7)	3.42	0.82
CH	(8)	5.22	−0.23
	(9)	5.31	0.00
	(10)	6.84	0.26
	(11)	7.25	
	(12)	8.50	−0.14

[a] The Δ values are normalized so that $\Delta(6) = 1.00$ ppm.

moiety surrounding a high-spin nickel(II) atom while the signal nos. (2), (4), (5) and (9) correspond to an AE entity linked to a diamagnetic nickel(II) atom. Furthermore, the initial δ values of the first set of signals are identical to those observed for [AENiImH] [17] so that we can reasonably conclude that in $\mathbf{B}_{22}$ the nickel atom which is able to bind pyridine is located in the outer site.

The signals with initial δ values of 6.84, 7.25 and 8.50 are attributed to the imidazole H(5) and H(4) and N=C*H*, respectively.

EPR Spectroscopy

In solution and at room temperature, all the spectra related to monometallic or homo- and heterobimetallic species, $\mathbf{A}_1$, $\mathbf{B}_{11}$, $\mathbf{B}_{12}$, $\mathbf{B}_{21}$ and $\mathbf{C}_1$ show hyperfine structures corresponding to a coupling to the copper nucleus. Superhyperfine structures only appear with heterobimetallic complexes, $\mathbf{B}_{12}$, $\mathbf{B}_{21}$ and $\mathbf{C}_1$. In these three cases, the second metallic centre is diamagnetic (Ni^{2+} or Zn^{2+}) so that we may consider that the copper centres are diluted in a diamagnetic matrix. This gives a good test for the formation and retention of the bimetallic imidazolate bridged structure in solution. In accordance with the presence of three nitrogen atoms in the coordination sphere of copper [19], seven superhyperfine lines are observed (Fig. 2). It may be noted that the corresponding constant A_N displays almost identical values in $\mathbf{B}_{12}$, $\mathbf{B}_{21}$ and $\mathbf{C}_1$, i.e. 12.7×10^{-3} cm^{-1}. Frozen solutions of the latter three species in non-coordinating solvents (CH_2Cl_2, acetone) give axial spectra with a low intensity of the parallel lines while the use of coordinating solvents (MeOH, DMSO) induces a better resolution of the $g_\parallel$ signals. A similar behaviour has been found with [AECuImNiAE]$^+$ [9], for which

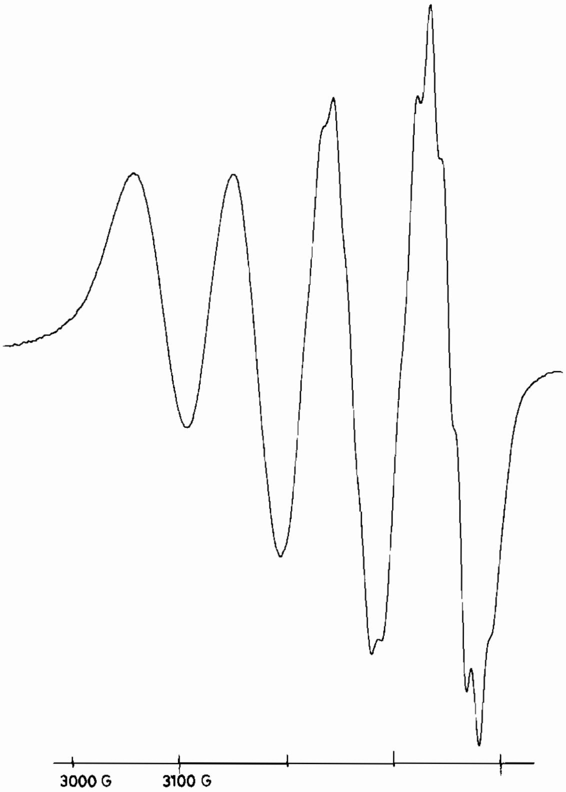

Fig. 2. ESR spectrum of $\mathbf{C}_1$.

the structural determination showed short intermolecular copper–copper distances (3.499(1) Å). So, in the solid state and in frozen solutions, dipolar intermolecular interactions between copper atoms are present. Thus for $\mathbf{C}_1$, the copper–zinc species, $\Delta M = \pm 2$ transitions appear as a well-defined seven-line pattern centered at 1540 gauss with an average spacing of 80 G. The $\Delta M_S = \pm 1$ region is more difficult to interpret since lines due to the doublet state and to the triplet state are overlapping. From these data, it appears that the copper–copper interactions, which lead to the formation of tetrametallic species, only occur to a limited extent in $\mathbf{C}_1$ while they are complete for $\mathbf{B}_{12}$ and $\mathbf{B}_{21}$. The reason for this difference may probably be found in the greater steric hindrance of $Zn(hfa)_2$ compared to M_0AE.

Solid state and frozen solutions spectra (CH_2Cl_2) of the monomeric species $\mathbf{A}_1$ give an isotropic signal centred at $g = 2.099$ showing that magnetic interactions are still operative. Methanolic frozen solutions give axial spectra with $g_\parallel > g_\perp$ and similar to those of the heterobimetallic species. g and A values are reported in Table 4.

Magnetic Susceptibility: Solid State and Solution

Magnetic susceptibility data were collected in the range 5–280 K for samples $\mathbf{A}_1$ and $\mathbf{B}_{11}$. In the case of $\mathbf{A}_1$, the data corrected for dimagnetism and TIP are

TABLE 4. EPR data

	g_{iso}	$A_{iso} \times 10^{-4}$ (cm^{-1})	$g_{\parallel}$	$A_{\parallel} \times 10^{-4}$ (cm^{-1})	Solvent
A_1	2.098 2.115	88.1	2.211	200.2	MeOH solid
$\mathbf{B}_{11}$	2.094 2.103	87.0			CH_2Cl_2 solid
$\mathbf{B}_{12}$	2.096	88.1	2.203	199.5	acetone
$\mathbf{B}_{21}$	2.101	86.3	2.212	200.3	acetone
$\mathbf{C}_1$	2.095	90.0	2.212	193.1	MeOH

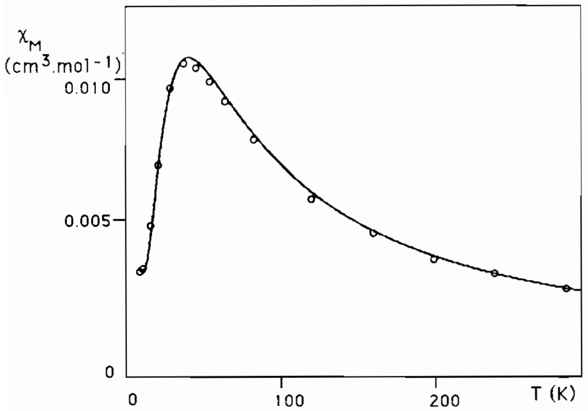

Fig. 3. Temperature dependence of the magnetic susceptibility for $\mathbf{B}_{11}$.

well represented by a Curie–Weiss law, $\chi_M^{corr} = C/(T - \theta)$ where $C = 0.39$ deg cm^3 mol^{-1} and $\theta = -2$ K. The non-zero value of θ is consistent with a weak intermolecular interaction. According to the molecular field approximation and with two interacting nearest neighbors for each metal centre, this θ value would give an approximate J value of -1.5 cm^{-1}.

A plot of χ_M versus T for complex $\mathbf{B}_{11}$ is represented in Fig. 3. The susceptibility goes through a maximum at *c.* 40 K, then decreases. This behaviour is typical of an antiferromagnetically coupled system. The absence of a Curie tail in the low temperature region indicates that the sample is free of paramagnetic mononuclear impurities. Therefore, the χ_M values may be fitted to the Bleaney–Bower expression for isotropic exchange in a copper(II) dimer without including a paramagnetic correction. The resulting values of g and $2J$ are 2.08 and -48 cm^{-1} ($g = 2.08 \pm 0.01$; $J = 48 \pm 2$ cm^{-1}), respectively. The best-fitted curve in Fig. 3 is represented by a solid line with $R = 6.4 \times 10^{-4}$ ($R = \Sigma(\chi_{obs} - \chi_{calc})^2/\Sigma(\chi_{obs})^2$. So, in the case of $\mathbf{B}_{11}$, the intermolecular contribution to the exchange process is virtually insignificant with respect to the intramolecular contribution mediated by the imidazolate ligand.

The mononuclear A_2 and dinuclear $\mathbf{B}_{22}$ nickel complexes are diamagnetic in the solid state and in solution in non-coordinating solvents. When a coordinating solvent (Py) is used, A_2 remains diamagnetic whereas $\mathbf{B}_{22}$ displays a paramagnetic behaviour. Room temperature measurements (Evans' method) yield an effective magnetic moment per molecular unit of 3.0 BM. Furthermore, nearly identical values of the moment at room temperature characterize solid samples of the heterobinuclear complexes $\mathbf{B}_{12}$ and $\mathbf{B}_{21}$ ($\mu = 1.9$ BM) and their solutions in acetone ($\mu = 1.9$ BM). On the contrary, a significant difference is observed between these two complexes when the moments are determined from solutions in pyridine: $\mu = 3.5$ BM for $\mathbf{B}_{12}$ and $\mu = 1.9$ BM for $\mathbf{B}_{21}$.

Electronic Spectra

The data reported in Table 5 reveal that the spectra of all the copper complexes under investigation are solvent dependent. Spectra of acetone solutions are almost identical with nujol mull spectra, except in the case of A_1. In this instance, the maximum of absorbance occurs at 600 nm for nujol mulls, 534 nm for acetone solutions and 590 nm for pyridine solutions. The last value is observed for all the copper complexes in pyridine solutions and may be considered as characteristic of a penta- or hexacoordinated copper centre [11]. In the solid state, such a coordination mode would imply a polynuclear chain structure through molecular interactions mediated by the nitrogen atom of imidazole not included in the coordination sphere. This explanation would be in line with the observation of a single isotropic signal in the EPR spectrum and with the structural determination of a similar complex [8]. In contrast to the behaviour of $\mathbf{B}_{11}$, the dinuclear complex $\mathbf{C}_1$ displays identical spectra for nujol mulls and acetone solutions. This can be considered as a

TABLE 5. Electronic spectra and magnetic data (solid state and solution)

Complexes	λ_{max} (nm)		Magnetic moment (293 K)		
	$(CH_3)_2CO$ or $CHCl_3$	C_5H_5N	Solid state	Solution $CHCl_3$	Solution C_5H_5N
A_1	534	590	[a]		
A_2	[b]	[b]	0[c]	0	0
$\mathbf{B}_{11}$	540, 570	595	[a]	2.4	2.4
$\mathbf{B}_{12}$	[b]	770, 820	1.8	1.9	3.4
$\mathbf{B}_{21}$	570	592	1.8	1.9	1.9
$\mathbf{B}_{22}$	[b]	774, 820	0	0	2.9
$\mathbf{C}_1$	538	600	1.8		
C_2	[b]	[b]	0		

[a] Antiferromagnetism, see text. [b] Not observed. [c] Diamagnetism.

proof of the existence of the heterodinuclear complex. Comparing the four copper complexes studied in acetone solutions leads to the conclusion that the ligand field experienced by the metal ion is effectively larger at the inner site (λ_{max} = 535 nm) than at the outer site which is characterized by a λ_{max} value of 560 nm.

As for the nickel complexes, a major difficulty arises from the fact that the d–d transitions associated with square planar geometry are expected around 450 nm where the absorptions due to charge transfer and/or ligand transitions are still important. Absorptions attributable to a nickel ion in octahedral symmetry are observed for pyridine solutions of complexes $\mathbf{B}_{12}$ and $\mathbf{B}_{22}$ where one nickel ion is in the outer site. It may be noted that the spectrum of $\mathbf{A}_2$, $\mathbf{B}_{21}$ and $\mathbf{C}_2$ where the nickel ion lies in the inner site does not comprise any absorption at *c.* 770 and 820 nm. These data are consistent with those related to the copper complexes. Both point to a significant difference of ligand fields between the inner and the outer site.

Discussion

All the experimental data show that the ligand AE-ImH primarily behaves as a tetradentate, dianionic Schiff base to yield mononuclear neutral copper(II) and nickel(II) entities containing a MN_3O chromophore. These mononuclear units possess a free coordination site, namely the outer nitrogen atom of the imidazole ring, which is immediately available for linking a second metal centre. This would yield three types of final products: (i) mononuclear complexes with a possible solvatation of the metal atoms; (ii) polynuclear complexes resulting from self-association of the mononuclear precursors; (iii) dinuclear complexes resulting from the reaction of the mononuclear units with coordinatively unsaturated complexes.

Spectroscopic and magnetic data show that process (ii) is likely operative for solid samples (and possibly frozen solutions in non-coordinating solvents) of CuAE-Im. In this instance each mononuclear unit would act as an axial ligand towards the copper atom of a second unit to yield a chain structure. However it may be noted that such a structure which implies penta (or hexa) coordinated metal centres is hardly compatible with the spectroscopic and magnetic properties of NiAE-Im. Therefore it is reasonable to assume that NiAE-Im actually is a mononuclear complex in the solid state and in solution as is CuAE-Im in solution. The third possibility is obviously illustrated by the obtention of complexes **B** and **C**.

In spite of many attempts, we did not succeed in preparing cationic mononuclear units in which the pyrrolic NH group would be non-deprotonated. This inclines us to think that in the MAE-Im units, the free site is actually a pyridinic nitrogen atom and that it preserves its pyridinic character when it coordinates a second metal ion. Such a model would be in line with the experimentally established non-equivalence of the inner and outer sites in the dinuclear complexes $[M_iAE\text{-}ImM_oAE]^+$.

In non-coordinating solvents, a copper ion in the inner site of a dinuclear complex is characterized by a λ_{max} of *c.* 535 nm which is identical to the value observed for the mononuclear complex CuAE-Im (534 nm) but very different from the value associated with the outer site, i.e. 570 nm. The latter value does not differ significantly from the values found for $[AECuPy]^+$ (568 nm) and $[AECuImH]^+$ (560 nm) where coordination of Py and ImH occurs via pyridinic nitrogen atoms. Conversely, the former value may be compared to that obtained for a genuine example of coordination through a deprotonated pyrrolic group, i.e. CuAE-Pyr with λ_{max} = 525 nm.

As for the nickel complexes, NMR data show that in presence of pyridine NiAE-Im remains low spin while in $[NiAE\text{-}ImNiAE]^+$, one nickel atom only, probably the outer one, adds pyridine and becomes high spin. This is substantiated beyond doubt by susceptibility measurements. Addition of pyridine transforms a low-spin nickel atom into a high-spin one only when it is located at the outer site, the inner site being occupied either by a second nickel atom which remains diamagnetic as it does in the mononuclear complex, or by a copper atom.

The difference between the two sites is strongly reminiscent of the difference previously observed between, on the one hand $[AENiPy]^+$ and $[AENiImH]^+$ which form diadducts with pyridine and, on the other hand NiAE-Pyr which remains diamagnetic in the presence of an excess of pyridine. This suggests that in the dinuclear complexes of the **B** type, the imidazolate ligand has a rather localized structure with two markedly different nitrogen atoms: a pyrrolic nitrogen at the inner site and a pyridinic nitrogen at the outer site. Such a situation is hardly conceivable for the symmetrical complex $[AENiImNiAE]^+$ in spite of the fact that the possibility of fixing pyridine is restricted to one metal centre. We have suggested that, in this case, the difference between the two sites is induced by the coordination of pyridine onto the first metal ion. This is probably the fundamental difference between the two types of complexes.

The magnetic properties of the polynuclear copper complexes deserve two particular comments. The magnitude of the antiferromagnetic interaction increases significantly on going from the associated form $(CuAE\text{-}Im)_n$ to the dinuclear complex $[CuAE\text{-}ImCuAE]^+$ ($\mathbf{B}_{11}$) even though, in both cases, the interaction is mediated by an imidazolate nucleus.

This is not unexpected since in the former species the bridge is from an equatorial to an axial coordination site whereas two equatorial sites are involved in the latter species. Due to the localization of the magnetic orbitals in the equatorial plane of each copper atom, it is obvious that the second geometry alone is able to allow a significant interaction.

Interestingly very similar values of the antiferromagnetic interaction are found for **B**$_{11}$ ($2J = -48$ cm^{-1}) and for [AECuImCuAE]$^+$ ($2J = -43$ cm^{-1}). However it is known that the presence of a substituent on the C_2 carbon of the imidazole ring prevents coplanarity of this ring with two equatorial planes which comprise the magnetic orbitals [10] so that we may conclude that the π orbitals of the imidazole are not involved in the coupling [20]. Due to the lack of structural data, a more detailed analysis of these magnetic data does not seem desirable.

References

1 L. Casella, *Inorg. Chem., 23* (1984) 2781.
2 G. Brewer and Ekk Sinn, *Inorg. Chim. Acta, 87* (1984) 241.
3 R. Atkins, G. Brewer, E. Kokot, G. M. Mockler and Ekk Sinn, *Inorg. Chem., 24* (1985) 127.
4 N. Matsumoto, J. Kanesaka, A. Ohyoshi, M. Nakamura, S. Kohata and H. Okawa, *Bull. Chem. Soc. Jpn., 60* (1987) 3056.
5 C. T. Brewer and G. Brewer, *J. Chem. Soc., Chem. Commun.*, (1988) 854.
6 N. A. Bailey, R. Bastida, D. E. Fenton, S. J. Lockwood and C. H. McLean, *J. Chem. Soc., Dalton Trans.*, (1988) 839.
7 N. Matsumoto, T. Akui, H. Murakami, J. Kanesaka, A. Ohyoshi and H. Okawa, *J. Chem. Soc., Dalton Trans.*, (1988) 1021.
8 N. Matsumoto, S. Yamashita, A. Ohyoshi, S. Kohata and H. Okawa, *J. Chem. Soc., Dalton Trans.*, (1988) 1943.
9 J.-P. Costes, J.-F. Serra, F. Dahan and J.-P. Laurent, *Inorg. Chem., 25* (1986) 2790.
10 J.-P. Costes, G. Commenges and J.-P. Laurent, *Inorg. Chim. Acta, 134* (1987) 237 and unpublished data.
11 J.-P. Costes and J.-P. Laurent, *Inorg. Chim. Acta, 134* (1987) 245.
12 G. Cros and J.-P. Costes, *C. R. Acad. Sci., Ser. B, 173* (1982) 294.
13 H. Adams, N. A. Bailey, I. S. Baird, D. E. Fenton, J.-P. Costes, G. Cros and J.-P. Laurent, *Inorg. Chim. Acta, 101* (1985) 7.
14 J.-P. Costes, *Transition Met. Chem., 10* (1985) 185.
15 J.-P. Costes, F. Dahan and J.-P. Laurent, *Inorg. Chem., 24* (1985) 1018.
16 D. F. Evans, *Proc. Chem. Soc.*, (1958) 115.
17 J.-P. Costes and J.-P. Laurent, unpublished work.
18 C. Srivanavit and D. G. Brown, *Inorg. Chem., 14* (1975) 2950.
19 A. K. Wiersma and U. J. Windle, *J. Chem. Phys., 68* (1964) 2316.
20 A. Bencini, C. Benelli, D. Gatteschi and C. Zanchini, *Inorg. Chem., 25* (1986) 398.